Electronic Power Waves in Networks of Inverters

Slobodan N. Vukosavic
Dept. of Electrical Engineering
The University of Belgrade
Belgrade, Serbia
boban@etf.rs

Aleksandar M. Stankovic
Dept. of Electrical and Computer Engineering
Tufts University
Medford, MA, USA
astankov@ece.tufts.edu

***Abstract*—The paper describes the phenomenon of electronic power waves in large networks of inverters. These waves have similarities with electromechanical waves that have been observed in actual electric power systems, and also have significant differences, including dependence on control tuning of inverters and on operating point. Electronic power waves are significantly faster than their electromechanical counterpart, but way below the speed of light. Analytical models are presented and illustrated by computer simulations. They provide a basis for further study of spatial phenomena in emerging inverter-rich power systems, made possible by new generations of sensors (such as phasor measurement units) equipped with very accurate time stamps.**

***Index Terms*—Power Electronic Converters, Power Grids, Inverters, Power system Dynamics, Power System Stability.**

I. INTRODUCTION

The study of spatial aspects of power system transients has a rich, fascinating history that intertwines conceptual advances with practical engineering concerns and solutions. The first paper proposing a detailed analytical model that we are aware of is [1]. Within a decade, authors of [2] arrived to a very similar model starting from practical stability concerns in the Western US interconnection. An influential sequence of papers started by [3] has generalized the models and analytical methods, and serves as a point of departure for most papers on the subject that followed. A recent two-part series [4-5] summarizes the theoretical aspects and explains their practical relevance in a sequence of examples. In this paper we present some preliminary modeling and control ideas for electronic power waves that are most aligned with [6]. The electromechanical waves predicted and later observed in actual power systems [1-6] can only be quantified in practice with high-bandwidth sensors. In the case of electronic power waves that we consider one would need input (kHz-sampled, unprocessed) samples in phasor measurement units (PMUs) [7,8] which have been appropriately time-stamped [9].

Conventional models of power system transients use nodal descriptions of components and interconnections, so spatial aspects of transients are hard to understand. With the adoption of grid-side inverters faster transient phenomena need to be described and stabilized. Under such circumstances, we believe that physics-based strategies are most promising in light of possibly complicated behavior of heterogeneous components. Time-horizons for stabilization that are of the order of milliseconds will likely result in stabilization policies that combine local and non-local (area-wide) components.

We are convinced that the study of electronic power waves is useful for understanding system-wide phenomena in large networks of inverter-connected sources and loads. Engineering applications of such studies will likely follow the path blazed by electromechanical dynamics, and will include stabilization and protection improvements in the near-term and event forensics and cyber-physical security in the longer-term. In addition, it is very likely that electromechanical and inverter-based sources and loads will co-exist in power systems for a long time to come, so there is definitely a need to understand their hybrid behavior.

II. DYNAMICS OF INDIVIDUAL GRID-SIDE CONVERTERS

In grid-connected converters, a phase-locked loop is used to synchronize the *d-q* frame to the line voltages. In balanced three-phase systems, the line voltage is represented by a revolving vector with the amplitude and frequency that correspond to the line-voltage, and with the spatial orientation determined by the phase of the line-voltage (φ_L in Fig. 1). With *d-q* frame synchronized with the line-voltage vector, and with the *q*-axis aligned with the line-voltage vector, the *q*-axis current of the grid-side converter controls the active power, while the *d*-axis power controls the reactive power (Fig. 1).

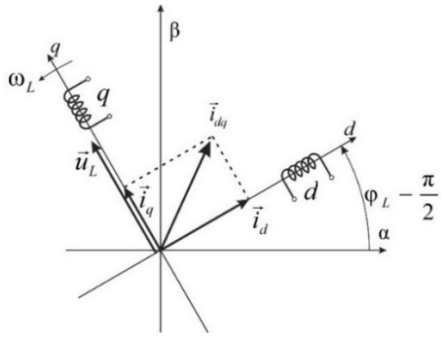

Fig. 1 Synchronization of the *d-q* frame to the line voltage [10].

978-1-5386-7138-2/18/$31.00 ©2018 IEEE

The use of the synchronous *d-q* frame in grid-side converters is often implemented via a simple and effective phase-detector. In Fig. 2, the *d-q* frame gets synchronized to the line voltage by the phase-locked loop. The position φ_{PLL} of the *q*-axis is obtained at the output of the PLL (Fig. 3). Assuming that the line voltage angle φ_L goes ahead of φ_{PLL} by $\Delta\varphi = \varphi_L - \varphi_{PLL}$, the line voltage vector advances with respect of the *q*-axis by the phase error $\Delta\varphi$. Therefore, the *d*-axis voltage component assumes a non-zero value, proportional to $-\sin(\Delta\varphi) \approx -\Delta\varphi$ for small angles. Thus, the *d*-axis voltage component is an indicator of the phase error, and the phase-detection is implemented in a straightforward way.

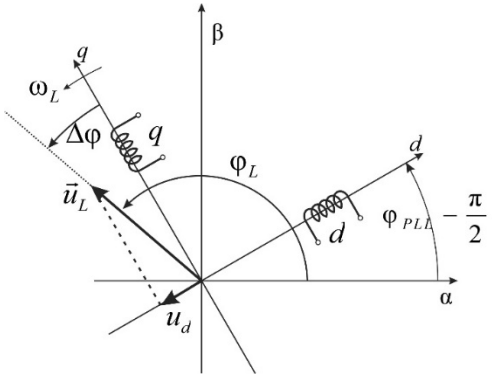

Fig. 2 The *d-q* frame based phase detector.

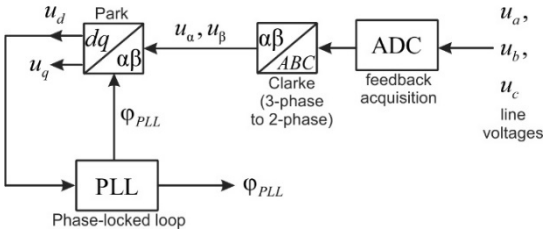

Fig. 3 The phase-locked loop (PLL).

The phase detector of Fig. 3 is represented by the gain block k_{PD} in the simplified diagram of the PLL (Fig. 4). With proportional and integral action of the controller, the driving signal is brought to the voltage controlled oscillator (VCO). Thus, the PLL output is

$$\varphi_{PLL}(s) = \left(\frac{k_{VCO} k_{PD} k_P}{s} + \frac{k_{VCO} k_{PD} k_i}{s^2} \right) \cdot \Delta\varphi(s) \qquad (1)$$

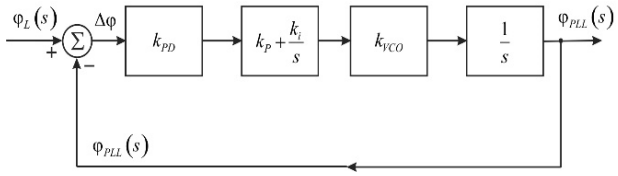

Fig. 4 Simplified block diagram of the PLL.

The power delivered by the grid-side inverter depends on the voltage amplitude, current amplitude and the angle between the voltage and current vectors,

$$P_G = |\vec{u}_L| \cdot |\vec{i}_{dq}| \cdot \cos(\Delta\varphi + \psi) = U \cdot I \cdot \cos(\Delta\varphi + \psi). \quad (2)$$

Transient changes of the line-voltage angle produce the phase error $\Delta\varphi$, which results transient changes of the inverter active power. For small changes of $\Delta\varphi$,

$$\Delta P_G = -U \cdot I \cdot \sin(\psi) \cdot \Delta\varphi = -Q_0 \cdot \Delta\varphi, \qquad (3)$$

where Q_0 is the reactive power delivered by the inverter. From (1), (3) and from Fig. 4,

$$\Delta P_G(s) = -\frac{Q_0 \cdot s^2}{s^2 + s \cdot k_P k_{PD} k_{VCO} + k_i k_{PD} k_{VCO}} \cdot \varphi_L(s). \quad (4)$$

It is of interest to study the propagation of the phase-shift and power disturbances along a sting of the grid-side inverters, as shown in Fig. 5, where φ_L is the line-voltage phase at the connection point of each inverter (e.g., $\varphi_{L,k}$ for the k-th inverter), P_G is the inverter active power, and P_{Load} is the local power consumption.

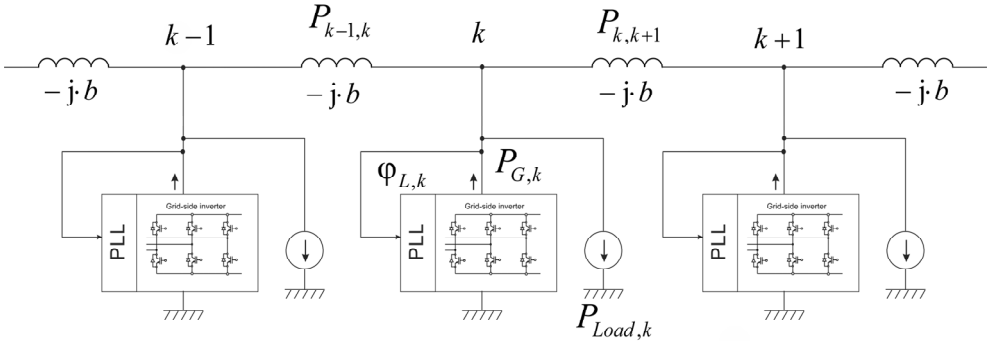

Fig. 5 A string of grid-side inverters.

III. Wave Propagation on a String of Inverters

Consider the case shown in Fig. 5 when many inverter/load cells are connected in a string, and, focusing on the power balance for the k-th cell

$$P_{G,k} - P_{Load,k} = P_{k,k+1} - P_{k-1,k} \quad (5)$$

Where $P_{G,k}, P_{Load,k}$ are power generated and consumed in the cell k, and $P_{k,k+1}$is the power flow between cells k and $k+1$. Let b be the susceptance of the line between any two cells

$$P_{k,k+1} = bV_kV_{k+1}\sin(\varphi_{L,k} - \varphi_{L,k+1}) \quad (6)$$

Which is well approximated for small angular differences with

$$P_{k,k+1} \approx bV_kV_{k+1}(\varphi_{L,k} - \varphi_{L,k+1}) \quad (7)$$

Thus the right-hand side of (5) becomes (assuming uniform voltage magnitudes along the string)

$$bV^2(2\varphi_{L,k} - \varphi_{L,k+1} - \varphi_{L,k-1}) \quad (8)$$

Next, we consider an incremental version of (6), and with assumed constant power load withing the cell $P_{Load,k}$ we get

$$\Delta P_{G,k} = bV^2(2\Delta\varphi_{L,k} - \Delta\varphi_{L,k+1} - \Delta\varphi_{L,k-1}) \quad (9)$$

We note that the term in the parentheses approximates the spatial derivative of the line voltage angle

$$\frac{\partial^2\Delta\varphi_L}{\partial x^2} \quad (10)$$

From the previous section we note the (second order) differential equation description of dynamics for φ_{PLL} in the forward branch; for compactness, we define gains $k_1 = k_P k_{PD} k_{VCO}$ and $k_2 = k_i k_{PD} k_{VCO}$. Then, multiplying that equation with $-Q_0$ (reactive power generation before the transient), we obtain

$$\frac{-Q_0}{k_2}\ddot{\varphi}_{PLL,k} + \frac{-Q_0}{k_1}\dot{\varphi}_{PLL,k} = \Delta P_{G,k} = bV^2\frac{\partial^2\Delta\varphi_L}{\partial x^2} \quad (11)$$

From the block diagram in the previous section we note that

$$\varphi_{L,k} = \varphi_{PLL,k} + \frac{1}{k_1}\dot{\varphi}_{PLL,k} + \frac{1}{k_2}\ddot{\varphi}_{PLL,k} \quad (12)$$

From the typical values for the constants $k_1, k_2$and from the fact that $\varphi_{L,k} = \varphi_{PLL,k}$ in steady state, we make the following approximation

$$\frac{\partial^2\Delta\varphi_L}{\partial x^2} \approx \frac{\partial^2\Delta\varphi_{PLL}}{\partial x^2} = \frac{\partial^2\varphi_{PLL}}{\partial x^2} \quad (13)$$

Which allows us to summarize our electronic power wave in a single equation

$$\frac{-Q_0}{k_2}\ddot{\varphi}_{PLL,k} + \frac{-Q_0}{k_1}\dot{\varphi}_{PLL,k} = bV^2\frac{\partial^2\varphi_{PLL}}{\partial x^2} \quad (14)$$

Please note that an analogous derivation can be made for two-dimensional grids as in [3]; similarly, one could model the inverter power deviation for large angular deviations, and restore the nonlinear model for power flows between cells. We aim to demonstrate that the linearized model shown above already has a wealth of relevant information. Note, however, that no such simplifications are used in simulations presented later. For example, following [3], we can estimate the velocity of the waves predicted by (14) as

$$v^2 = \frac{k_2 bV^2}{|Q_0|} \quad (15)$$

Note that the velocity depends on the control gain k_2, on the operating point Q_0 , and on the line parameters. To get a rough estimate, consider a (very long) string at 220kV, with line reactance at 0.4 Ω/km and the base power of 100MVA (so Z_{Base} = 484 Ω), as in [3]. Then, to get the pre-transient power flow of the order of 1 p.u. and the overall phase difference of 2π, we consider the case of 60 sections, each approximately 120 km long, so that in (14) b =10 p.u. and V = 1p.u. For $k_2 = (2\pi)^2$, so that the closed-loop bandwidth of the PLL is 1Hz [10], and Q_0 =-1 in per unit, we get the speed of ≈ 20 sections per second or ≈ 2400 km/s.

Please note that this estimate is approximately five times faster than in the case of electromechanical waves [2,3,6]. On the other hand, the range of velocities is broader than in the case of electromechanical waves, as the control settings of k_2 and the operating point Q_0 are likely to vary widely. If the overhead lines were to be replaced with cables at the same voltage, the susceptance b would increase 3-4 times. At the same time, Q_0 which depends on both line parameters and load characteristics, would also be affected, most likely upward. Note that Q_0 = 0, which makes the speed estimate (15) unbounded, signals a modeling issue more than a true singularity, as it models all inverters as constant power sources. Given our assumption about constant power loads, that would mean that a power disturbance propagates instantaneously due to power balance in each cell.

IV. Simulation Results

The string of grid inverters (Fig. 5) comprising a total of 64 inverters is modeled and simulated. The gains within PLL units of grid inverters are set to achieve the closed loop bandwidth of 1 Hz. The initial net power increment at each node is set to zero, and the line frequency is set to the nominal value (50 Hz). It is assumed that the voltages along the string retain their rated value (1 p.u.), and that the transmission line reactance between the two inverters is 0.1 p.u. (b = 10 p.u.), as shown in Fig. 5. In Fig. 6, a total of 64 inverters are connected in series. The input disturbance is applied to the leftmost node in the form of a 500 ms wide power pulse having an amplitude of 1 p.u. The rightmost node could either be left open, or supplied by the impedance-matching power source [6] that quenches the reflection of the electronic power waves. Reactive power of each inverter is set to Q_0 = 1 p.u.

Simulation results shown in Fig. 7 present the change of the line-voltage phase at the connection points of corresponding inverters in the case when the string end on the right is left opened. It takes roughly 2.5 seconds for the wave

to reach the end of the string. With $f = 50$ Hz and $x_l \Delta = 0.1$ p.u, the distance between two inverters is $\Delta = 100$km (so the string length is roughly $L = 100 \times 64 = 6400$ km), which corresponds to the speed of $v = 2560$ km/s, an estimate in agreement with (11), where the square of the speed is reciprocal to the reactive power of inverters. In Fig. 7, reflected electronic power waves clearly contribute to the overall oscillatory nature of the transient.

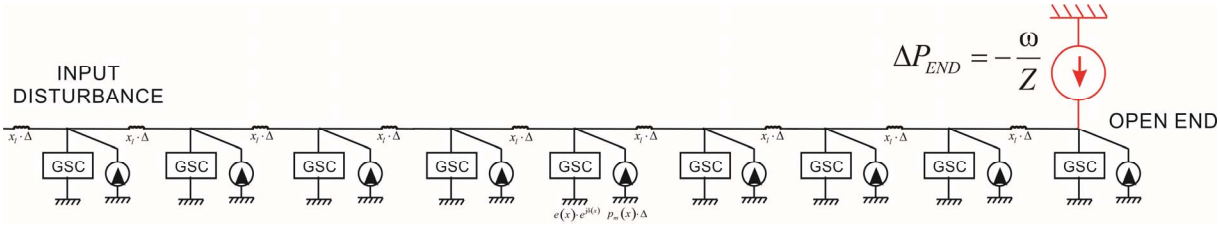

Fig. 6. A total of 64 inverters (GCS) are connected in series. The input disturbance is applied to the leftmost node in the form of a 500 ms wide power pulse. The rightmost node could be left open, or, supplied by the impedance-matching power source that quenches the reflection of the electronic power waves.

Simulation results given in Fig. 8 are obtained by adding the wave-quenching compensation. The compensation is applied at the right end of the string, and it provides the power pulse that rests in proportion with the phase-shift deviation. Reflection at the right end of the string is suppressed, as well as the oscillations of the line-voltage phase-shift and active power. It is also of interest to estimate the required power and energy rating of the wave-quenching device at the end of the line. To that aim, the power supplied from the compensator is plotted in Fig. 9. The waveform represents the power drawn from the wave-quenching compensator at the end of the line, and it is obtained simultaneously with the results plotted in Fig. 8. The peak power remains below 0.2 p.u., while the positive pulse dwells for less than 2 seconds.

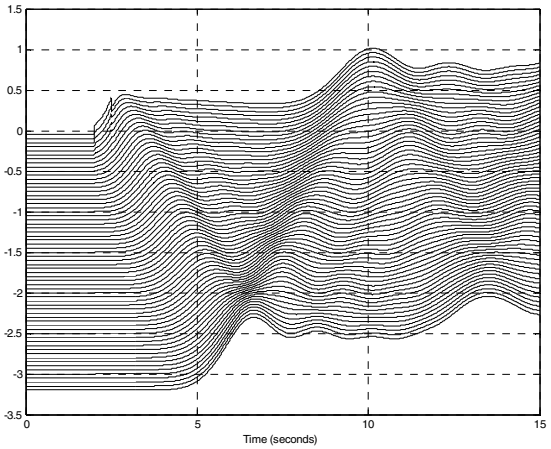

Fig. 7. The power pulse of 1 p.u. and 500 ms is supplied from the left. The right end of the string is left open. The waveforms represent the line-voltage phase shift at connection points. The waveforms are intentionally scale-shifted in vertical direction.

From the analytical considerations and simulation results, we note wave phenomena can occur in networks of inverters just as electromechanical waves have been observed on networks with conventional synchronous generators. While the speed of electromechanical waves is of the order of 500 km/s, the speed of electronic power waves in the case of grid-side inverters is considerably higher (likely 5 times or more). Dynamic phenomena in an ac network with grid-side converters is largely affected by control settings, such as the PLL, and by reactive loading of the inverters (which depends on actual loads and on transmission line parameters). The quenching of the waves requires some means of local energy storage, as we discuss below.

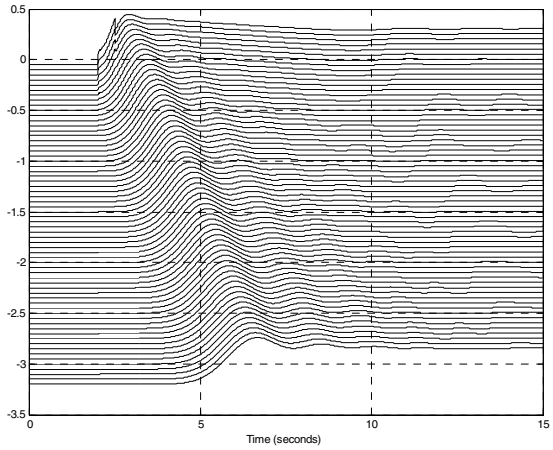

Fig. 8. In addition to settings of Fig. 7, the impedance-quenching compensation is applied at the right end of the string, providing the power pulse that rests in proportion with the phase-shift deviation.

Finally, we consider example of a power system in which both electromechanical and electronic power waves can co-exist. We connect in a ring structure a string with grid-side inverters (top portion of Fig. 10) with a string with conventional electromechanical sources (bottom portion of Fig. 10). Each string has 64 sections, with electromechanical parameters as in [6]. The initiating event is the same as in Figs. 7-8, and it occurs at a junction of two strings.

In Fig. 10 we observe that the wave propagates much faster through the top (inverter) portion than through the bottom (synchronous generator) portion. We also note numerous

reflections occurring at the two connection points between strings.

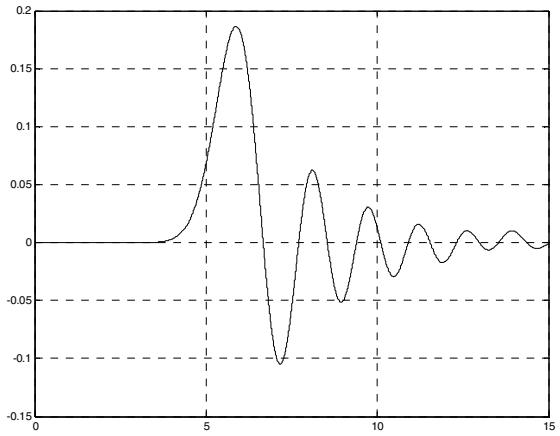

Fig. 9. The power drawn from the wave-quenching compensator at the end of the line, obtained simultaneously with the results plotted in Fig. 9.

The wave-quenching compensator has to supply the transient power pulses that are illustrated in Fig. 9. With the pulse width below 2 seconds, the required energy storage is $W_{es} = 2 \cdot P_{nom}$, where P_{nom} is the rated power of the inverter. Conventional 3-phase inverters with capacitor-supported dc-bus have a rather limited internal energy storage. With the allowed change of the dc-bus voltage of 20%, the transient power P_{nom} cannot be maintained over the pulse dwells longer than 5-10 ms. In order to upgrade a grid-side inverter into a wave-quenching device, it is necessary to provide the means for considerably larger energy storage, capable of a near-unlimited number of charging cycles. This would eliminate any form of batteries available today. A suitable topology enhancement of grid-side inverters that is based on super-capacitors and the switching power interface are shown in Fig. 11.

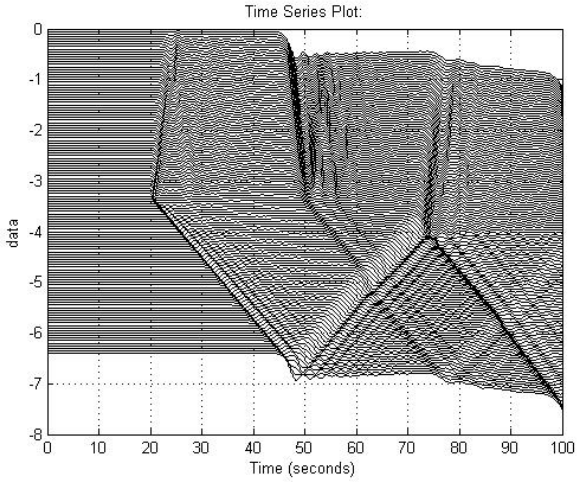

Fig. 10. A ring structure with grid-side inverters (half-ring, top portion) and conventional electromechanical sources (half ring, bottom portion).

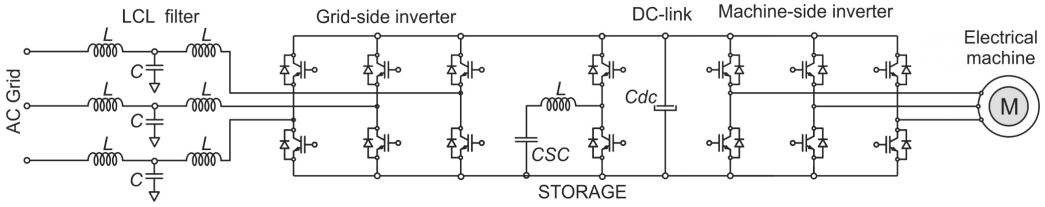

Fig. 11. Topology enhancement of grid-side inverters that permits local energy storage for the wave-quenching power compensator. The *storage* block comprises the super-capacitor *CSC* and the switching power interface.

V. CONCLUSIONS

In this paper we argue for the existence of electronic power waves in cases with networked inverters. Our main tool is an idealized continuum model in the form of a wave equation. We use simulations with discrete cells to establish credibility predictions of the continuum model. Such models are a primary means for understanding spatial aspects of disturbance propagation in power systems. In particular, they bring to the fore global (or at least non-local) facets of transient behavior. These are hard to grasp from traditional descriptions, which capture nodal dynamics at a fixed location. Electronic power waves have similarities with electromechanical waves, but also display some key differences. The fact that electronic waves are faster is not very surprising, as inverters tend to have faster dynamics than traditional generators. However, electronic waves also depend strongly on control settings and on the operating point. One implication for system protection in networks of inverters is that some decisions will likely remain local. The stabilization via feedback control will have to take into account spatial and temporal properties of electronic power waves. In that regard, physics will continue to provide the much needed guidance in terms of compensation strategy and energy storage requirements.

Future studies on electronic power waves will likely use more detailed inverter and load representations and spatially irregular connections. While we do not expect that detailed inverter models will fundamentally change the main findings reported here, the role of different network topologies needs to be examined and quantified. Another intriguing direction is the study of power systems with mixed electromechanical and electronic power waves, as illustrated in our final simulation example.

REFERENCES

[1.] A. Semlyen, "Analysis of disturbance propagation in power systems based on a homogenous dynamic model," *IEEE Trans. Power App. Syst.*,vol. PAS-93, no. 2, pp. 676–684, Mar. 1974.

[2.] R. L. Cresap and J. F. Hauer, "Emergence of a new swing mode in the western power system," *IEEE Trans. Power App. Syst.*, vol. PAS-100, no. 4, pp. 2037–2045, Apr. 1981.

[3.] J. S. Thorp, C. E. Seyler, and A. G. Phadke, "Electromechanical wave propagation in large electric power systems," *IEEE Trans. Circuits Syst. I, Fundam. Theory Appl.*, vol. 45, no. 6, pp. 614–622, Jun. 1998.

[4.] T. Li, G. Ledwich, Y.Mishra, J. Chow, and A. Vahidnia, ''Wave Aspect of Power System Transient Stability—Part I: Finite Approximation'', *IEEE Trans. Power Systems*, vol. 32, No. 4, pp. , 2493-2500, July 2017.

[5.] T. Li, G. Ledwich, Y.Mishra, J. Chow, and A. Vahidnia, ''Wave Aspect of Power System Transient Stability—Part II: Control Implications'', *IEEE Tran. Power Systems*, vol. 32, No. 4, pp. , 2501-2508, July 2017.

[6.] B. C. Lesieutre, E. Scholtz, and G. C. Verghese, "A zero-reflection controller for electromechanical disturbances in power networks," in *Proc. 14th Power Syst. Comput. Conf.*, Sevilla, Spain, 2002, pp. 1–7.

[7.] IEEE Standard for Synchrophasor Measurements for Power Systems, IEEE Power and Energy Society, IEEE Std C37.118.1TM-2011 and IEEE Std C37.118.1aTM-2014.

[8.] M.K. Penshanwar, M. Gavande, M.F.A.R. Satarkar, "Phasor Measurement Unit Technology and its Applications: A Review," International Conference on Energy Systems and Applications (ICESA), Nov. 2015.

[9.] A. Traub-Ens, J. Bordoy, J. Wendeberg, L.M. Reindl, and C. Schindelhauer, "Data Fusion of Time Stamps and Transmitted Data for Unsynchronized Beacons", *IEEE Sensors J.*, vol. 15, no. 10, pp. 5946-5953, Oct. 2015.

[10.] S.N. Vukosavic, *Grid Side Converters -Design and Control*, Springer, 2018.